

# Sympathetic cooling of bosonic and fermionic Lithium gases towards quantum degeneracy

F. Schreck, G. Ferrari, K. L. Corwin, J. Cubizolles, L. Khaykovich, M.-O. Mewes and C. Salomon  
*Laboratoire Kastler Brossel, Ecole Normale Supérieure, 24 rue Lhomond, 75231 Paris CEDEX 05, France*  
(October 25, 2018)

Sympathetic cooling of two atomic isotopes is experimentally investigated. Using forced evaporation of a bosonic  ${}^7\text{Li}$  gas in a magnetic trap, a sample of  $3 \cdot 10^5$   ${}^6\text{Li}$  fermions has been sympathetically cooled to  $9(3) \mu\text{K}$ , corresponding to  $2.2(0.8)$  times the Fermi temperature. The measured rate constant for 2-body inelastic collisions of  ${}^7\text{Li}$   $|2, 2\rangle$  state at low magnetic field is  $1.0_{-0.5}^{+0.8} 10^{-14} \text{ cm}^3 \text{ s}^{-1}$ .

PACS numbers: 05.30.Fk, 05.30.Jp, 03.75.-b, 05.20.Dd, 32.80.Pj

In atomic physics, the combination of laser cooling and evaporative cooling in magnetic traps has been successfully used to reach Bose-Einstein condensation in dilute vapors [1,2]. These techniques, however, are not universal. Producing laser light at appropriate wavelengths is sometimes difficult and laser cooling of molecules remains a challenge. Relying on elastic collisions [3], evaporative cooling fails for fermions at low temperature. Indeed no  $s$ -wave scattering is allowed for identical fermions and when the temperature  $T$  decreases, the  $p$ -wave cross-section vanishes as  $T^2$  [4].

Sympathetic cooling allows one to overcome these limitations. It uses a buffer gas to cool another species via collisions and was first proposed for two-component plasmas [5]. Often used for cooling ions confined in electromagnetic traps [6,7], it has been applied recently to cool neutral atoms and molecules via cryogenically cooled Helium [8]. Sympathetic cooling using  ${}^{87}\text{Rb}$  atoms in two different internal states has led to the production of two overlapping condensates [9]. For fermions, the  $s$ -wave scattering limitation was overcome by using two distinct Zeeman substates, both of which were evaporatively cooled. This method has been used to reach temperatures on the order of  $\sim 300 \text{ nK} \sim 0.4 T_F$  [10], where  $T_F$  is the Fermi temperature below which quantum effects become prominent. Cold collisions between  ${}^6\text{Li}$  and  ${}^7\text{Li}$  were analyzed theoretically in [11] and it was predicted that sympathetic cooling of  ${}^6\text{Li}$  by contact with  ${}^7\text{Li}$  should work efficiently.

In this Letter, we report on the experimental demonstration of sympathetic cooling of  ${}^6\text{Li}$  fermions via collisions with evaporatively cooled  ${}^7\text{Li}$  bosons in a magnetic trap. Both species were cooled from  $2 \text{ mK}$  to  $\sim 9(3) \mu\text{K}$ , corresponding to  $T \sim 2.2(0.8) T_F$  where  $T_F = (\hbar\bar{\omega}/k_B)(6N)^{1/3}$ ,  $\bar{\omega}$  is the geometric mean of the three oscillation frequencies in the trap and  $N$  is the number of fermions. For these experimental conditions,  $T_F \sim 4 \mu\text{K}$ . This method represents a crucial step towards the production of a strongly degenerate Fermi gas of  ${}^6\text{Li}$  and the study of its optical and collisional properties [12,13]. It also opens the way to interesting studies on mixtures of Bose condensates and Fermi gases [14–16]. Finally  ${}^6\text{Li}$  is considered a

good candidate for the observation of BCS transition [17–19].

A sketch of our apparatus is shown in Fig.1. First the  ${}^7\text{Li}$  and  ${}^6\text{Li}$  isotopes are simultaneously captured from a slowed atomic beam and cooled in a magneto-optical trap (*MOT*) at the center of a Vycor glass cell [20]. On top of this cell is located a small appendage of external dimensions  $20 \times 7 \times 40 \text{ mm}$  and a wall thickness of  $2 \text{ mm}$ . The small dimension along  $y$  permits the construction of a strongly confining Ioffe-Pritchard (*IP*) trap using electro-magnets. The 2D quadrupole field is created by four copper Ioffe bars (*IB*), each consisting of three conductors running at a maximum current of  $700 \text{ A}$ . Axial confinement is provided by two pinch coils (*PC*) in series with two compensation coils (*CC*) at  $500 \text{ A}$  in order to reduce the bias magnetic field. For these currents, the radial gradient is  $2.38 \text{ kG/cm}$  and the axial curvature is  $695 \text{ G/cm}^2$ . With a bias field of  $15 \text{ G}$ , the trap frequencies for  ${}^7\text{Li}$  are  $\omega_{\text{rad}}/2\pi = 2.57(4) \text{ kHz}$  and  $\omega_{\text{ax}}/2\pi = 118(1) \text{ Hz}$ . The background-limited trap lifetime is  $130 \text{ s}$ . Atoms are transferred from the *MOT* region to the *IP* trap in a magnetic elevator quadrupole trap. The elevator consists of lower quadrupole (*LQ*) coils, (identical with the *MOT* coils) and upper quadrupole (*UQ*) coils centered on the *IP* trap axis,  $50 \text{ mm}$  above the *LQ* trap center. The current ratio between the two sets of coils determines the center of the resulting quadrupole trap, allowing the atoms to be lifted by adjusting this ratio.

This trap design allows both large compression and high atom numbers, two crucial parameters for evaporative cooling. This is particularly important for lithium atoms since the  $s$ -wave cross-sections at zero energy are at least 16 times smaller than for  ${}^{87}\text{Rb}$ . The scattering length for  ${}^7\text{Li}$  in state  $|F = 2, m_F = 2\rangle$  used in our experiments is  $-27a_0$  [21]. Finally, all coil currents can be switched off rapidly, allowing the potentials to be turned off non-adiabatically for time-of-flight absorption imaging. In contrast, early BEC experiments with  ${}^7\text{Li}$  used a permanent magnet trap [22].

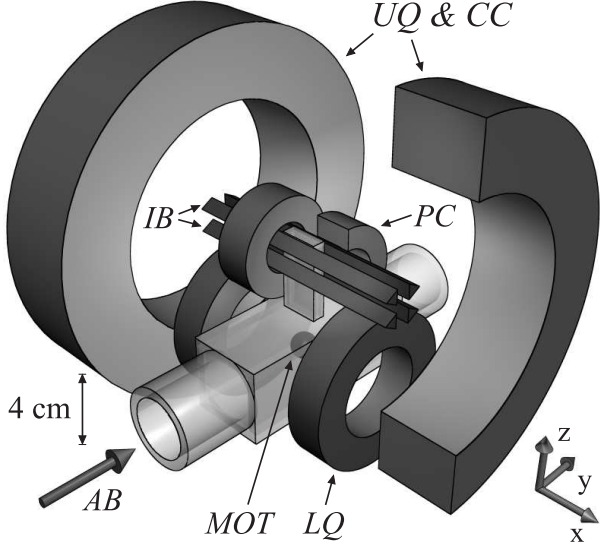


FIG. 1. Experimental set-up. Both lithium isotopes are collected from a slow atomic beam (AB) in a magneto-optical trap (MOT) at the center of a glass cell. Atoms are magnetically elevated using lower quadrupole (LQ) and upper quadrupole (UQ) coils into a small appendage. At this site, a strongly confining Ioffe-Prichard trap consisting of 4 Ioffe bars (IB), two pinch coils (PC) and two compensation coils (CC) allows evaporative cooling of  ${}^7\text{Li}$  to quantum degeneracy and sympathetic cooling of  ${}^6\text{Li}$ - ${}^7\text{Li}$  mixtures.

We describe now the main steps of our sympathetic cooling experiments (parameters are summarized in Table 1).  $6 \cdot 10^9$   ${}^7\text{Li}$  and  $1.6 \cdot 10^8$   ${}^6\text{Li}$  atoms are captured in  $\sim 1$  minute in the MOT. The relative numbers of  ${}^7\text{Li}$  and  ${}^6\text{Li}$  can be adjusted by changing the light intensity tuned to each isotope with the laser set-up described in [23]. Both isotopes are cooled to  $\sim 0.8$  mK, optically pumped to the upper hyperfine state,  $F=2$  (resp.  $F=3/2$ ) and captured in the LQ trap with an axial gradient of 400 G/cm. Characterization of the LQ trap with  ${}^7\text{Li}$  revealed two time scales for trap losses: a fast one (100 ms) that we attribute to spin relaxation and a slow one (50 s) due to Majorana transitions near the trap center. Just before the magnetic elevator stage about 40% of both isotopes remain trapped.

The transfer to the UQ trap is done by increasing the current in the UQ coils to 480 A in 50 ms and ramping off the current in the LQ coils in the next 50 ms. Nearly mode-matched transfer into the IP trap is accomplished by simultaneously switching on the IB and the pinch coils PC while switching off the UQ coils. The transfer efficiency from LQ trap to the IP trap is 15% and is limited by the energy cut due to the narrow dimension of the appendage (3 mm) in radial direction. High energy atoms hit the glass cell and are lost. A wider appendage would allow a higher transfer efficiency but at the expense of a reduced radial gradient. Our simulation shows that the chosen size is optimum with respect to the initial collision rate in the IP trap for a temperature of 1 mK in the LQ trap.

After compressing the IP trap to maximum currents and reducing the bias field to 15 G, we obtain  $2.5 \cdot 10^8$   ${}^7\text{Li}$  atoms and  $1.8 \cdot 10^7$   ${}^6\text{Li}$  atoms at a temperature of 7(3) mK. In these conditions, we have been unsuccessful in reaching runaway evaporation (i.e. increase of collision rate) on  ${}^7\text{Li}$  in presence or in absence of  ${}^6\text{Li}$ . Because the  $|2, 2\rangle$  state of  ${}^7\text{Li}$  has a negative scattering length, as the collision energy increases, the scattering cross-section falls to zero. This occurs at  $T_o = 4$  mK, i.e. within the  $s$ -wave energy range [24]. To overcome this limitation, we apply a stage of 1-dimensional Doppler cooling of  ${}^7\text{Li}$  in the IP trap with a bias field of 430 G using a  $\sigma^+ - \sigma^+$  laser standing wave aligned along the  $x$ -axis. Each beam has an intensity of  $25 \mu\text{W}/\text{cm}^2$  and is detuned about one natural linewidth below the resonance in the trap. In 1 s of cooling, the temperature in all three dimensions drops by a factor of 4 and the loss of atoms is 15%. In the compressed IP trap, the temperature is now  $\sim 2$  mK, sufficiently below  $T_0$ . Thus at the start of the evaporation, the collision rate is  $\sim 15 \text{ s}^{-1}$ , i.e. 2000 times the background gas collision rate.

Absorption images are taken with  $10 \mu\text{s}$  exposure time, immediately after the trap is turned off and before the cloud can expand. Independent laser systems provide isotope selective probe beams. From these images, the total number of atoms is found, to an accuracy of a factor of 2. The temperature is then deduced from a fit of the cloud size in the axial direction by a Gaussian of standard deviation  $\sigma_{\text{ax}}$  and the measured oscillation frequency  $\omega_{\text{ax}}$ . This temperature measurement agrees to within 15% with a time-of-flight measurement of the kinetic energy.

Evaporation is performed exclusively on  ${}^7\text{Li}$ . We apply a tunable microwave field near the  ${}^7\text{Li}$  hyperfine transition at 803.5 MHz to couple the  $|F=2, m_F=2\rangle$  trapped state to the  $|F=1, m_F=1\rangle$  untrapped state. To verify the effectiveness of the evaporation process, we first cool  ${}^7\text{Li}$  alone in the trap down to the regime of quantum degeneracy; after 15 s of compression of the cloud with a microwave knife fixed at 5.4 mK, we have  $2 \cdot 10^8$  atoms at a temperature of 1.2 mK [25]. We then lower the microwave cut energy from this value to  $\sim 5 \mu\text{K}$  in 45 s. The central phase space density is  $\rho_0 = n_0 \Lambda^3$  where  $\Lambda = h(2\pi mk_B T)^{-1/2}$  and  $n_0$  is the peak density. In Fig. 2,  $\rho_0$  is plotted vs atom number at various stages of the evaporation scan.  $\rho_0(N)$  is well fitted by a line of slope  $-2$  on a log-log scale, indicating a nearly constant collision rate during forced evaporation. We reached phase-space densities exceeding 2.6 with  $5 \cdot 10^4$  atoms at 1.2  $\mu\text{K}$ , meeting the condition for Bose-Einstein condensation. However, due to the effective attractive interaction, the trapped condensate is expected to be stable only for atom numbers up to a critical value [26,27] which, in our trap geometry, is  $\sim 600$ . Our current imaging system is unable to detect such a small sample. We also observe that the trap lifetime is reduced to 22(4) s at a peak density of  $4 \cdot 10^{12}$  at/cm $^3$  and a temperature

of  $21 \mu\text{K}$ , well above BEC. We attribute this reduction to dipolar relaxation and obtain a dipolar relaxation rate  $\beta_{7-7} = 1.0_{-0.5}^{+0.8} 10^{-14} \text{ cm}^3\text{s}^{-1}$  in agreement with the theoretical value  $1.6 10^{-14} \text{ cm}^3\text{s}^{-1}$  predicted in [28] and comparable to that measured in high magnetic field [29,30].

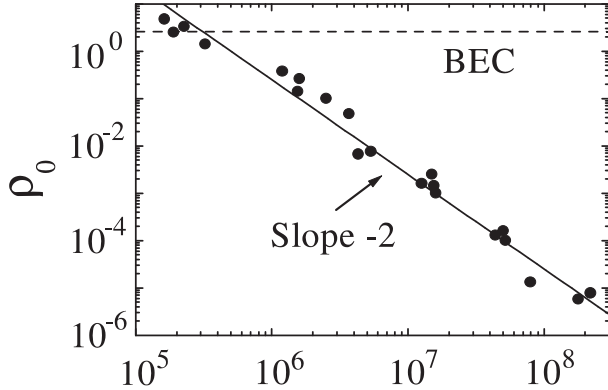


FIG. 2.  ${}^7\text{Li}$  peak phase-space density *vs* number of atoms  $N$  during single-species evaporation.

Using a similar evaporation ramp lasting 40 s with  $2.5 10^6$   ${}^6\text{Li}$  atoms and  $3.2 10^8$   ${}^7\text{Li}$  atoms, sympathetic cooling of fermionic  ${}^6\text{Li}$  is clearly shown in Fig.3. The displayed images recorded at various stages of the evaporation ramp for mixtures (a and b) or for  ${}^7\text{Li}$  alone with identical initial number (c). In (a), the optical density of the  ${}^6\text{Li}$  cloud is seen to increase considerably because of the reduction in size without apparent loss of atoms, a signature of sympathetic cooling. Comparisons of the cloud sizes between (a) and (b) indicate that  ${}^6\text{Li}$  and  ${}^7\text{Li}$  are in thermal equilibrium, except for the end of the evaporation. At 39 s,  ${}^6\text{Li}$  is at  $40 \mu\text{K}$ ,  ${}^7\text{Li}$  is not detectable (b), while  ${}^7\text{Li}$  alone is at  $20 \mu\text{K}$  (c). This indicates that between 36 and 39 s, the numbers of  ${}^6\text{Li}$  and  ${}^7\text{Li}$  have become equal. Beyond this point, the temperature of  ${}^6\text{Li}$  no longer decreases significantly. The thermal capacity of  ${}^6\text{Li}$  soon exceeds that of  ${}^7\text{Li}$ , resulting in heating and loss of  ${}^7\text{Li}$  during the final stage of forced evaporation (b). Under the same conditions but without  ${}^6\text{Li}$ , normal evaporative cooling of  ${}^7\text{Li}$  proceeds to a temperature of  $18 \mu\text{K}$  (c) which is below that obtained for  ${}^6\text{Li}$  at 39 s,  $35 \mu\text{K}$  (a).

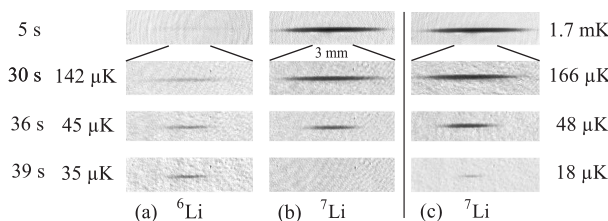


FIG. 3. Images of  ${}^6\text{Li}$  and  ${}^7\text{Li}$  atom clouds at various stages of sympathetic cooling (a, b) and during single-species evaporation (c) with identical initial numbers of  ${}^7\text{Li}$  atoms. Top images are 1 cm long, the others 3 mm. Temperatures of  ${}^6\text{Li}$  (resp.  ${}^7\text{Li}$  alone) are given on the left (right).

More quantitatively, temperatures and numbers of  ${}^6\text{Li}$  and  ${}^7\text{Li}$  atoms as a function of the microwave cut energy are plotted in Fig.4. Above  $40 \mu\text{K}$ , the temperature of all three clouds are nearly identical, indicating that the collision cross-section between the  ${}^7\text{Li}$   $|2, 2\rangle$  and  ${}^6\text{Li}$   $|\frac{3}{2}, \frac{3}{2}\rangle$  is not significantly smaller than that of the  ${}^7\text{Li}$   $|2, 2\rangle$  with itself. This is consistent with the prediction that the scattering length between these states of  ${}^6\text{Li}$  and  ${}^7\text{Li}$  is  $(40.8 \pm 0.2) a_0$  [11]. In addition, close thermal contact implies that the microwave knife acts the same on the  ${}^7\text{Li}$  cloud with or without  ${}^6\text{Li}$  present, as expected because the  ${}^6\text{Li}$  number is initially a very small fraction of the  ${}^7\text{Li}$  number. The ratio between the measured temperatures and the microwave cut energy is 4. At a temperature around  $35 \mu\text{K}$ , the number of  ${}^7\text{Li}$  atoms ( $N_7$ ) has been reduced to the number of  ${}^6\text{Li}$  atoms ( $N_6$ ). As a result the  ${}^6\text{Li}$  cloud is no longer cooled and remains at  $35 \mu\text{K}$ .

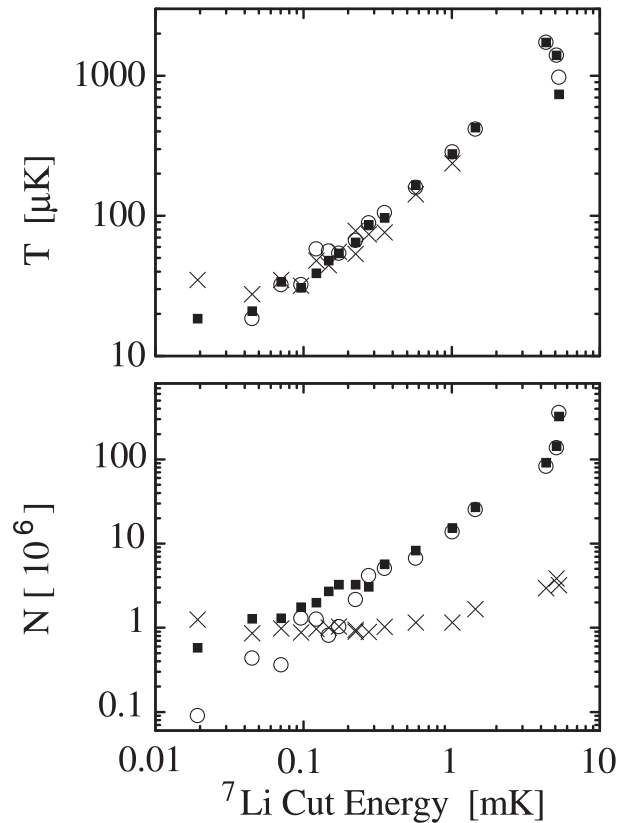


FIG. 4.  ${}^6\text{Li}$  (crosses) and  ${}^7\text{Li}$  (open circles) temperatures and numbers as a function of the  ${}^7\text{Li}$  cut energy. During sympathetic cooling, temperatures are the same down to a decoupling region below which  ${}^6\text{Li}$  is no longer cooled. Black squares show  ${}^7\text{Li}$  alone with identical parameters. Uncertainty in the  $x$ -axis is about 0.01 mK.

For classical gases, the decoupling temperature  $T_D$  is reached when  $N_7 \approx N_6$ . In the case of  ${}^7\text{Li}$  alone,  $T_7$  is approximately proportional to  $N_7$  and so  $T_D \propto N_6$ . Since  $T_F \propto N_6^{1/3}$ , the degeneracy parameter  $T_D/T_F \propto N_6^{2/3}$ , and Fermi degeneracy can be approached by reducing the number of  ${}^6\text{Li}$ . Doing this, the highest degeneracy reached after a complete sympathetic

cooling evaporation ramp was  $T/T_F = 2.2(0.8)$  at a temperature of  $9(3)\mu\text{K}$  with  $1.3 \cdot 10^5$   ${}^6\text{Li}$  atoms. At this stage we are limited by the detection efficiency of our imaging system.

Finally an important question for studies of mixtures of these degenerate gases is the possibility of inter-species loss mechanisms. We have searched for such losses by recording the  ${}^6\text{Li}$  trap lifetimes in presence and in absence of  ${}^7\text{Li}$  atoms at a peak density  $n_0({}^7\text{Li}) = 2 \cdot 10^{11} \text{at}/\text{cm}^3$  and a common temperature of  $530 \mu\text{K}$ . With  $n_0({}^7\text{Li}) = 4.6 n_0({}^6\text{Li})$ , the lifetimes were respectively  $73(10)\text{s}$  and  $73(8)\text{s}$ , showing no significant difference. We deduce an upper limit for dipolar decay rates,  $\beta_{6-7} \leq 1 \cdot 10^{-13} \text{cm}^3\text{s}^{-1}$ ,  $\beta_{6-6} \leq 4.6 \cdot 10^{-13} \text{cm}^3\text{s}^{-1}$ .

In summary we have demonstrated sympathetic cooling of fermionic lithium via evaporation performed on the bosonic Li isotope and obtained temperatures of  $2.2(0.8)T_F$ . Several improvements of the experiment should allow us to achieve full Fermi degeneracy and investigate the properties of such a quantum gas and of degenerate Boson-Fermion mixtures.

We are grateful for experimental assistance of Fabrice Gerbier and A. Sinatra, to ANDOR technology for loaning us a camera and to J. Dalibard, C. Cohen-Tannoudji, G. Shlyapnikov and D. Guéry-Odelin for discussions. M.-O.M., F.S., and K.C. were supported by a Marie-Curie Research fellowship of the EU, by a doctoral fellowship from the DAAD and by MENRT. This work was partially supported by CNRS, Collège de France, DRED, and the EC (TMR Network No. ERB FMRX-CT96-0002). Laboratoire Kastler Brossel is *Unité de recherche de l'École Normale Supérieure et de l'Université Pierre et Marie Curie, associée au CNRS*.

	${}^7\text{Li}$		${}^6\text{Li}$
	N	T [mK]	N
Compressed MOT	$6 \cdot 10^9$	0.8	$1.6 \cdot 10^8$
Lower Quadrupole	$2.5 \cdot 10^9$	1	$8 \cdot 10^8$
Capture I-P trap	$3.8 \cdot 10^8$	0.7	$1.3 \cdot 10^7$
Compressed I-P	$3.2 \cdot 10^8$	2	$2.5 \cdot 10^6$
End symp. cool.	$1.7 \cdot 10^6$	0.03	$1.2 \cdot 10^6$

TABLE I. Typical atom numbers and temperatures before and during sympathetic cooling

- 
- [1] M.H. Anderson *et al.*, Science **269**, 198 (1995).
  - [2] Proc. of the Int. School of Phys. "Enrico Fermi", M. Inguscio, S. Stringari and C. Wieman eds, (IOS Press, Amsterdam 1999).
  - [3] H.F. Hess, Phys. Rev. B **34**, 3476 (1986).
  - [4] B.DeMarco *et al.*, Phys. Rev. Lett. **82**, 4208 (1999).
  - [5] L. Spitzer *Physics of Fully Ionized Gases* (Interscience, New York, 1962).
  - [6] R.E. Drullinger *et al.*, Appl. Phys. **22**, 365 (1980).
  - [7] D.J. Larson *et al.*, Phys. Rev. Lett. **57**, 70 (1986).
  - [8] J. Kim *et al.*, Phys. Rev. Lett. **78**, 3665 (1997).
  - [9] C.J. Myatt *et al.*, Phys. Rev. Lett. **78**, 586 (1997).
  - [10] B. DeMarco and D.S. Jin, Science **285**, 1703 (1999).
  - [11] F.A. VanAbeelen, B.J. Verhaar, and A.J. Moerdijk, Phys. Rev. A **55**, 4377 (1997).
  - [12] B. DeMarco and D.S. Jin, Phys. Rev. A **58**, 4267 (1998).
  - [13] G. Ferrari, Phys. Rev. A. **59**, R4125 (1999).
  - [14] L. Viverit, C.J. Pethick and H. Smith, Phys. Rev. A **61** 053605 (1999) and references therein.
  - [15] K. Molmer, Phys. Rev. Lett. **80**, 1804 (1998).
  - [16] W. Geist, L. You and T. A. Kennedy, Phys. Rev. A, **59**, 1500, (1999)
  - [17] H. T. Stoof *et al.*, Phys. Rev. Lett. **76**, 10 (1996).
  - [18] R. Combescot, Phys. Rev. Lett. **83**, 3766 (1999).
  - [19] M. Houbiers and H.T.C. Stoof, Phys. Rev. A **59**, 1556 (1999).
  - [20] M.-O. Mewes, G. Ferrari, F. Schreck, A. Sinatra and C. Salomon, Phys. Rev. A **61**, 011403(R) (1999).
  - [21] E.R.I. Abraham, C.A. Sackett, and R.G. Hulet, Phys. Rev. A **R55**, 3299, (1997).
  - [22] C.C. Bradley *et al.*, Phys. Rev. Lett. **75**, 1687 (1995).
  - [23] G. Ferrari, M.-O. Mewes, F. Schreck, and C. Salomon, Opt. Lett. **24**, 151 (1999).
  - [24] J. Dalibard in [2].
  - [25] This compression phase was not used in  ${}^6\text{Li}$  cooling.
  - [26] P.A. Ruprecht *et al.*, Phys. Rev. A **51**, 4704 (1995).
  - [27] C.C. Bradley, C.A. Sackett, and R.G. Hulet, Phys. Rev. Lett. **78**, 985 (1997).
  - [28] A.J. Moerdijk and B.J. Verhaar, Phys. Rev. A **53**, R19 (1996).
  - [29] J.M. Gerton, C.A. Sackett B.J. Frew, and R.G. Hulet, Phys. Rev. A **59**, 1514 (1999).
  - [30] the definition of  $\beta$  is given by  $\dot{N} = -\beta n_0 N / \sqrt{2} - \alpha N$